Journal of Sciences, Islamic Republic of Iran 19(3): 247-260 (2008) http://jsciences.ut.ac.ir
University of Tehran, ISSN 1016-1104

Gold Distribution in Porphyry Copper Deposits of Kerman Region, Southeastern Iran

B. Shafiei[1,*] and J. Shahabpour[2]

[1] *Department of Geology, Gorgan University of Agriculture Sciences and Natural Resources, Gorgan, Islamic Republic of Iran*
[2] *Department of Geology, Shaheed Bahonar University of Kerman, Kerman, Islamic Republic of Iran*

Abstract

Gold contents of the Kerman porphyry copper deposits are generally low, ranging from 0.010 to 0.190 g/t. The copper ores exhibit Cu/Au atomic ratios much greater than 40000, and Au/Mo ratios below 30, which signifies them as gold-poor porphyry copper deposits. The gold-poor signature of the Kerman deposits complies with features such as higher contents of chalcopyrite and pyrite over bornite and magnetite in the hypogene ores, widespread phyllic and argillic alterations, weak correlations between Au and Cu, poor correlations between Au and Mo, and their association with adakitic-like intrusions derived from partial melting of the lower crustal rocks at a thickened continental arc. These features reflect rather low temperature (less than 600°C) and low oxygen fugacity of the primary ore-forming fluids involved in the formation of the Kerman porphyry copper deposits, indicating the low solubility of gold in low temperature fluids in comparison with higher temperature (~700°C) and more oxidized fluids responsible for the formation of gold-rich porphyry copper deposits. Present study indicates that a strong positive correlation exists between the gold and the magnetite contents of the porphyry copper deposits. These relationships indicate that deposits with higher gold and magnetite contents (*e.g.* Sar Kuh, Meiduk and Abdar), were emplaced at higher crustal levels and formed from more oxidized fluids in comparison to the gold-poor deposits (*e.g.* Sar Cheshmeh). These features can be used as exploration tools for identification of the gold-rich porphyry copper deposits in the porphyry copper metallogenic provinces.

Keywords: Gold; Porphyry Cu deposits; Kerman; Iran

Introduction

Most porphyry copper deposits contain some gold as by-product [1-6]. The average gold contents of the porphyry copper deposits is rather low, between 0.012 to 0.38 g/t [4,7]; however the huge tonnages of porphyry deposits provide a sizeable resource of gold with a significant economic value [5]. Several studies

* Corresponding author, Tel.: 09133432822, Fax: +98(171)4427040, E-mail: behnam.shafiei@gmail.com

have been carried out in the field of gold mineralization in the porphyry copper deposits worldwide [1-4,6,8,9-12]. Sillitoe [3] suggested that the border line for Au content in gold-rich porphyry copper deposits is about 0.4 g/t. Based on the Au/Mo ratios, Cox and Singer [4] divided the porphyry copper deposits into three groups: (1) porphyry Cu-Au deposits (Au/Mo>30); (2) porphyry Cu-Au-Mo deposits (3<Au/Mo<30); and (3) porphyry Cu-Mo deposits (Au/Mo<3). Kirkham and Sinclair [13] defined gold-rich porphyry copper deposits as those with Cu(wt.%)/Au(g/t) atomic ratios below 31,000. Based on the available data from many porphyry copper deposits, Kesler *et al.* [6] suggested a Cu(wt.%)/Au(g/t) ratio of about 40000 as a boundary for discriminating between gold-rich and gold-poor porphyry copper deposits. Several studies indicated that the gold content in porphyry copper deposits is controlled by factors such as tectonic setting, depth of emplacement, and the ore-forming fluid characteristics [1-6,10-12].These factors along with other characteristics such as the ore tonnage, morphology, and the age of the ore deposits have been used to distinguish between different types of porphyry copper deposits (*e.g.* porphyry Cu-Mo, and porphyry Cu-Au deposits).

The distribution of gold in the porphyry copper deposits of Iran, and the factors controlling the gold contents, are poorly understood. To this aim, we selected eight porphyry copper deposits from the Kerman region, which is known as the most important porphyry Cu-bearing metallogenic province in Iran [14,15]. The variations of Au, Mo and Cu are used to examine the gold distribution and its metallogenic importance in these deposits.

The Kerman porphyry copper region with several deposits such as Sar Cheshmeh, Meiduk, Darreh Zar, Now Chun, Sar Kuh, Dar Alu as well as many smaller and sub-economic reserves (Table 1) [15-22] have been developed in a volcano-plutonic assemblage, 40-50 km wide and over 400 km long [15,23-26] in southeastern segment of the central Iran Cenozoic magmatic arc (Urumieh-Dokhtar belt) (Fig. 1). It is generally accepted that this magmatic arc has been generated in response to successive stages of the Tethyan ocean closure during Paleogene and a continent-continent collision in late Paleogene-Neogene between Arabian plate and Central Iran micro-plate [27-31]. Genetically, porphyry copper mineralization in the Kerman region is associated with Miocene- Pliocene porphyritic stocks [19-21,32,33], known as the Kuh-Panj type granitoids [23]. The ore-hosting intrusions are porphyritic in texture and vary in composition from diorite to quartz diorite, granodiorite, and locally quartz monzonite [18,20,21,34]. The rocks are per-aluminous (Fig. 2a) and all belong to the I-type magnetite granitoid series (Fig. 2b) [25,26]. The Kerman ore-hosting porphyries display geochemical features comparable to those of the adakitic rocks (Fig. 2c), such as high Na_2O contents (3.5-4.8 wt. %), high Sr (≥400 ppm), low Y (≤18 ppm), high Sr/Y (>40), strong REE fractionation (Yb=0.36-1.5 ppm;La/Yb=19-53), slightly positive Eu anomalies($Eu/Eu^* \geq 1$), and relatively non-radiogenic Sr isotopic signatures ($^{87}Sr/^{86}Sr$= 0.704253-0.704800) [25,26]. The ore-related granitoids are characterized as orogenic granitoids rather than fractionated granitoids (Fig. 2d), and mostly belong to a post-collisional environment rather than a pre-plate collision tectonic setting (Fig. 2e) [25,26]. This is consistent with the lack of a subduction zone during the Neogene time beneath central Iran micro-continent [27-31]. The adakitic-like signatures displayed by the ore-related granitoids are suggestive of the presence of high pressure hydrous magmas derived from partial melting of a source with residual amphibole+garnet typical of compressional tectonic regimes, and continental crust >40km thick, rather than subducting hot slab melting (Fig. 2f) [25,26].

Most of the porphyritic intrusions are associated with well-developed potassic (K-feldspar and biotite), sodic (albite), sericitic, silicic, propylitic, and locally argillic hydrothermal alterations [18,20,21,34]. The mineralization occurs as quartz stockworks, veins, and disseminated sulfides in both the host stock and the older volcanic and pyroclastic rocks [18,20,21,25,26, 35]. The common hypogene ore minerals are chalcopyrite, pyrite, and subordinate molybdenite; bornite and magnetite are scarce. A common feature in the Kerman porphyry copper deposits, is the occurrence of mineralized and barren dykes [18,20,21] and breccia pipes [36]. The supergene oxidation and secondary Cu-enrichment occurred in all the deposits; but it is only well-developed in the giant and large deposits, such as Sar Cheshmeh, Meiduk, and Darreh Zar.

Materials and Methods

For the present study, a database, consisting of Au (g/t), Mo (%), and Cu (%) assays for 106 hypogene ores from drill cores and outcrops of eight porphyry copper deposits in the Kerman region was established (Table 2). Large samples (~3 kg) from ores with potassic and phyllic alteration were prepared by jaw-crushing (≤12.7 mm), followed by grinding in a Cr-steel ring mill (≤20 μm) in the Sar Cheshmeh Copper Complex. Representative samples were analyzed for Au, Mo, and Cu at the Central Laboratory of the Sar Cheshmeh Copper Complex. Gold was analyzed by Graphite Furnace Atomic Absorption Spectroscopy technique

Table 1. The summary of location, reserve, grade and size of some porphyry copper deposits in Kerman region

Ore deposit	Geographic location	Reserves and grades	Ore deposit size	References
Sar Cheshmeh	Pariz area 29° 56′ N 55° 52′ E	1200Mt, 0.7%Cu, 0.03%Mo,	Giant size (~8,400,000t of fine Cu)	[14,17,24,66]
Meiduk (Lachah)	Shahr Babak area 30° 20′ N 55° 10′ E	150Mt, 1.15%Cu	Large size (~1,725,000t of fine Cu)	[17,24,66]
Darreh Zar	Pariz area 29° 51′ N 55° 53′ E	49Mt, 0.64%Cu, 0.004%Mo	Medium size (~317,000t of fine Cu)	[17,24]
Now Chun	Pariz area 29° 55′ N 55° 51′ E	80Mt, 0.32%Cu	Medium size (~256,000t of fine Cu)	[17,24]
Iju	Dehaj area 30° 33′ N 54° 57′ E	25Mt, 0.46%Cu	Medium size (~115,000t of fine Cu)	[17,24]
Dar Alu	Sarduieyh area 29° 25′ N 57° 06′ E	18Mt, 0.47%Cu	Small size (~84,600t fine Cu)	[17,24]
Sar Kuh	Pariz area 29° 55′ N 57° 46′ E	16Mt, 0.46%Cu	Small size (~64,000t of fine Cu)	[17,24]
Bagh Khoshk	Pariz area 29° 33′ N 55° 58′ E	24Mt, 0.27%Cu	Small size (~64,800t containing Cu)	[17,24]

(GFAAS) with a detection limit of 0.01 ppm, after pre-concentration by a Lead Fire Assay technique (LFA) from 25 gr samples. Mo and Cu contents were measured by Direct Current Plasma technique (DCP) with a detection limit of 5 ppm, and Atomic Absorption Spectroscopy technique (AAS) with a detection limit of 10 ppm, respectively. Also, forty two samples from potassic zones were examined for magnetite contents (wt.%), as an index for the oxygen fugacity of the primary ore-forming fluids, by a magnetic scale (SATMAGAN analyzer, Model 135, Corrigan Canada Ltd.) after induction of electromagnetic field on sample cell at the Central Laboratory of Sar Cheshmeh Copper Complex. saturation magnetization measurements of samples were achieved through the amount of handle's movement by the magnetic force applied on. The obtained data from these movements were multiplied by the coefficient obtained from the SATMAGAN analyzer calibration curve which was achieved through measuring standard samples; and therefore the magnetite content of the samples was determined. The magnetite content (wt.%) of these samples was also measured by quantitative microscopic analysis (particle size distribution) on powder samples at the Laboratory of mineralogy in Sar Cheshmeh Copper Complex. The values obtained from this method were close to those resulted from the SATMAGAN analyzer. Analytical data are presented in Table 2.

Results

Gold content in the hypogene-ore samples is generally low, ranging from 0.010 to 0.190 g/t. The highest average gold content of about 0.09 g/t, was obtained from Sar Kuh deposit (Table 3). Molybdenum contents in the samples range between 0.0001% and 0.196 % (Table 3). The Sar Cheshmeh samples show the highest Mo contents. Distribution of the elements in the variably altered and mineralized samples, indicate that the highest gold contents occur in the potassic ores which are affected by strong phyllic alteration. In contrast, the highest Mo grades are associated with potassic alteration. There is a weak correlation between Au and Cu (r=0.3) in the ore samples from the potassic zone (Fig. 3); however, the Au contents show no correlation with Cu and Mo in the phyllic zone (Figs. 4 and 5). The Mo values indicate a strong positive correlation with Cu (r=0.7) in the potassic zones, but do not show positive relationship with Cu in the phyllic zones (Figs. 3, 4 and 5).

The Kerman porphyry copper deposits exhibit low Au/Mo ratios (≤9); the highest values are obtained from the Sar Kuh deposit (27) (Table 3). The Cu/Au atomic ratios are much greater than 40,000 (Table 3). Accordingly, the Kerman deposits are typical of gold-poor porphyry copper deposits. Furthermore, the porphyry copper deposits of the Kerman region mostly plot in the Au-poor (porphyry Cu-Mo or PCD-Mo) and the Au-Mo bearing (porphyry Cu-Au-Mo or PCD-Au-Mo) fields of the Cox and Singer's diagram (Fig. 6). They plot entirely below the lines of Au-rich porphyry copper deposits, close to the porphyry copper deposits of the Chilean Andes and the North American Cordillera, as defined by Sillitoe [3] and Kirkham and Sinclair [13] (Fig. 7). Exceptionally, Sar Kuh plots within the field of Au-rich porphyry copper deposits (porphyry Cu-Mo or PCD-Au) as defined by Cox and Singer [4] (Fig. 6). However, the mean gold content of the deposits (~0.19 g/t) is lower than the average gold content of the gold-rich porphyry deposits (≥0.4 g/t). This is due to the lower Cu and Mo contents compared

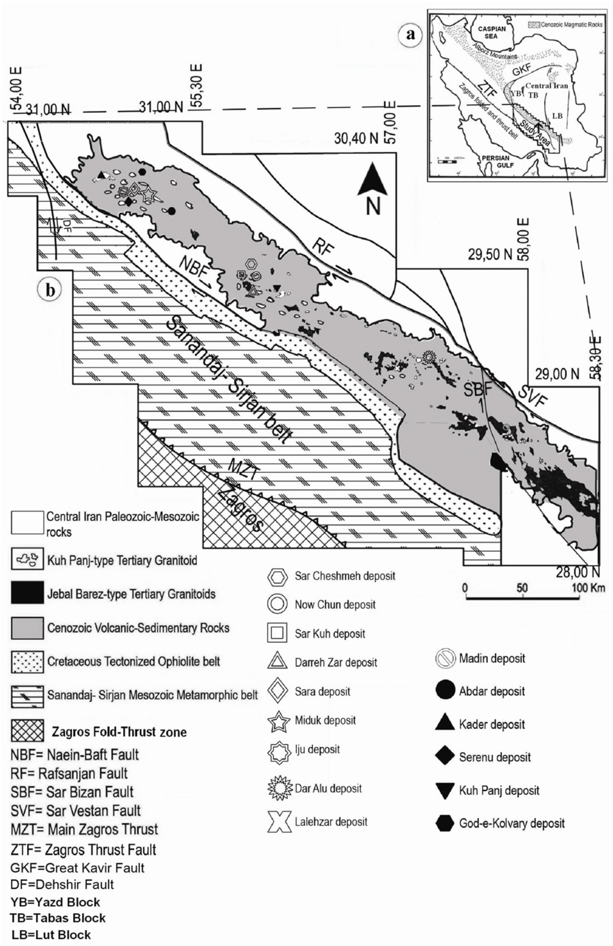

Figure 1. (a) Map showing the regional distribution of the Urumieh-Dokhtar magmatic arc and location of the Kerman porphyry copper region in southeast Iran, (b) simplified tectonic map of the Kerman porphyry copper region showing the three main litho-tectonic zones, regional distribution of granitoid groups and porphyry copper deposits (modified from Rio Tinto Ltd. [15]; Dimitrijevic [23]).

with other porphyry copper deposits of the Kerman region.

Discussion

The reasons for the low Au-content of the Kerman porphyry copper deposits are discussed below.

Ore-Forming Fluid Characteristics

In most porphyry copper systems, gold is closely

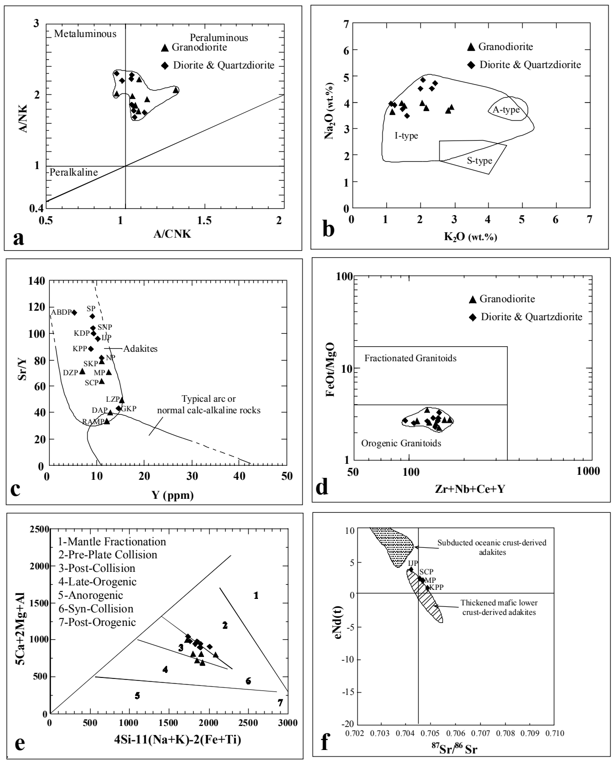

Figure 2. Geochemical and tectonic classification of the Cu-hosting porphyries from Kerman region: (a) A/NK vs. A/CNK diagram [A/NK=molar Al_2O_3 / (Na_2O+K_2O); A/CNK= molar Al_2O_3 / (CaO+Na_2O+K_2O)] [67], (b) - Na_2O vs. K_2O diagram [68], (c) Y vs. Sr/Y diagram [69] showing adakitic affinity of the Neogene Cu-hosting porphyries from the Kerman region. SCP= Sar Cheshmeh porphyry stock; MP= Meiduk porphyry stock; DZP= Darehzar porphyry stock; SKP= Sar Kuh porphyry stock; SP= Sara porphyry stock; IJP= Iju porphyry stock; SNP= Serenu porphyry stock; GKP= God-e-Kolvary porphyry stock; KDP= Kader porphyry stock; NP= Now Chun porphyry stock; DAP= Dar Alu porphyry stock; ABDP=Abdar porphyry stock; LZP= Lalleh Zar porphyry stock; RAMP= Razi Abad-Madin porphyry stock; KPP= Kuh Panj porphyry stock, (d) FeOt vs. Zr+Nb+Ce+Y diagram [70], (e) 4Si-11(Na+K) -2(Fe+Ti) versus 5Ca+2Mg+Al [71], (f) Plots of εNd vs. $^{87}Sr/^{86}Sr$ for ore-hosting porphyries from the Kerman porphyry copper belt. Fields for adakites is derived from Wang et al. [72].

Table 2. Au, Mo, Cu, and Magnetite contents of ore samples from the porphyry copper deposits of Kerman region

Sample No.	Deposit	Depth of sampling (Bore hole/outcrop)	Ore-type	Cu (%)	Mo (%)	Au (g/t)	Fe_3O_4 (%)
AB-1	Abdar	BH-AB3;185-186m	Potassic	0.23	0.001	0.040	0.69
AB-2	Abdar	BH-AB3;268m	Potassic	0.20	0.010	0.050	0.81
AB-3	Abdar	BH-AB3;274m	Potassic+Phyllic	0.32	0.040	0.090	0.86
AB-4	Abdar	BH-AB5;79.5-81.5m	Phyllic+Argillic	0.31	0.014	0.080	-
AB-5	Abdar	BH-AB5;81.5-83m	Phyllic+Argillic	0.28	0.015	0.070	-
AB-6	Abdar	BH-AB3;119-121m	Potassic+Phyllic	0.29	0.012	0.070	0.75
AB-7	Abdar	BH-AB3;130m	Potassic+Phyllic	0.31	0.008	0.060	0.79
AB-8	Abdar	BH-AB3;121-122.5m	Potassic+Phyllic	0.36	0.011	0.090	0.86
AB-9	Abdar	BH-AB3;259-261.5m	Potassic+Phyllic	0.35	0.009	0.090	0.94
AB-10	Abdar	BH-AB5;86-88m	Phyllic+Argillic	0.30	0.009	0.080	-
DA-1	Dar Aloo	BH-D2;50-73m	Phyllic+Argillic	0.50	0.010	0.030	-
DA-2	Dar Aloo	BH-D2;120-125m	Phyllic+Argillic	0.70	0.009	0.040	-
DA-3	Dar Aloo	BH-D2;160-186m	Phyllic+Argillic	0.14	0.012	0.010	-
DA-4	Dar Aloo	BH-D2;192-196m	Phyllic+Argillic	0.17	0.001	0.020	-
DA-5	Dar Aloo	Outcrop	Phyllic+Argillic	0.56	0.008	0.040	-
DA-5	Dar Aloo	Outcrop	Phyllic+Argillic	0.49	0.006	0.040	-
DA-6	Dar Aloo	Outcrop	Phyllic+Argillic	0.42	0.005	0.030	-
DA-7	Dar Aloo	Outcrop	Phyllic+Argillic	0.53	0.004	0.040	-
SR-1	Sara	BH-49;514m	Phyllic+Argillic	0.25	0.003	0.030	-
SR-2	Sara	BH-49;533-536m	Phyllic+Argillic	0.39	0.003	0.040	-
SR-3	Sara	BH-49;553m	Phyllic+Argillic	0.28	0.013	0.030	-
SR-4	Sara	BH-49;558m	Phyllic+Argillic	0.40	0.007	0.050	-
SR-5	Sara	BH-49;562m	Phyllic+Argillic	0.25	0.008	0.020	-
SR-6	Sara	BH-49;568m	Phyllic+Argillic	0.59	0.001	0.040	-
SR-7	Sara	BH-49;575m	Phyllic+Argillic	0.51	0.002	0.040	-
SR-8	Sara	Outcrop	Phyllic+Argillic	0.36	0.004	0.030	-
SR-9	Sara	Outcrop	Phyllic+Argillic	0.35	0.003	0.030	-
SR-10	Sara	Outcrop	Phyllic+Argillic	0.34	0.002	0.030	-
SK-1	Sar Kuh	BH-S11;182m	Potassic	0.21	0.004	0.050	0.97
SK-2	Sar Kuh	BH-S11;174m	Potassic	0.21	0.003	0.060	0.98
SK-3	Sar Kuh	BH-S11;163m	Potassic+Phyllic	0.41	0.003	0.190	1.86
SK-4	Sar Kuh	BH-S11;146m	Potassic+Phyllic	0.36	0.002	0.110	1.28
SK-5	Sar Kuh	BH-S11;120m	Potassic+Phyllic	0.36	0.002	0.070	1.42
SK-6	Sar Kuh	BH-S11;106m	Potassic+Phyllic	0.41	0.002	0.060	0.93
SK-7	Sar Kuh	BH-S11;98m	Potassic+Phyllic	0.39	0.002	0.070	1.48
SK-8	Sar Kuh	BH-S11;72m	Potassic+Phyllic	0.33	0.003	0.070	0.99
SK-9	Sar Kuh	BH-S11;56m	Phyllic+Argillic	0.29	0.003	0.060	-
SK-10	Sar Kuh	Outcrop	Phyllic+Argillic	0.35	0.002	0.090	-
MP-1	Meiduk	BH-44;820-825m	Potassic	0.60	0.008	0.060	0.86
MP-2	Meiduk	BH-44;733-739m	Potassic+Phyllic	0.78	0.006	0.070	0.79
MP-3	Meiduk	BH-55;752-755m	Potassic+Phyllic	0.85	0.007	0.050	0.80
MP-4	Meiduk	BH-55;698-702m	Potassic+Phyllic	0.73	0.006	0.060	0.82
MP-5	Meiduk	BH-56;652-660m	Potassic+Phyllic	0.68	0.007	0.050	0.83
MP-6	Meiduk	BH-56;714-720m	Potassic+Phyllic	0.96	0.004	0.070	0.71
MP-7	Meiduk	BH-53;220-225m	Potassic+Phyllic	0.74	0.006	0.050	0.72
MP-8	Meiduk	Outcrop	Phyllic+Argillic	0.49	0.005	0.030	-
MP-9	Meiduk	Outcrop	Phyllic+Argillic	0.41	0.004	0.040	-
MP-10	Meiduk	Out crop	Phyllic+Argillic	0.43	0.004	0.050	-
SDP-1	Seridun	BH-S1;220-234m	Phyllic	0.25	0.010	0.020	-
SDP-2	Seridun	BH-S1;193-200m	Phyllic	0.26	0.012	0.020	-
SDP-3	Seridun	BH-S1;205m	Phyllic	0.28	0.017	0.030	-
SDP-4	Seridun	BH-S1;359m	Phyllic	0.19	0.009	0.020	-

Table 2. Continued

Sample No.	Deposit	Depth of sampling (Bore hole/outcrop)	Ore-type	Cu (%)	Mo (%)	Au (g/t)	Fe_3O_4 (%)
SDP-5	Seridun	BH-S1;178-185m	Phyllic	0.31	0.007	0.030	-
SDP-6	Seridun	BH-S1;234-246m	Phyllic	0.24	0.013	0.020	-
SDP-7	Seridun	BH-S1;200-209m	Phyllic	0.26	0.011	0.030	-
SDP-8	Seridun	BH-S1;185-193m	Phyllic	0.31	0.010	0.020	-
DZP-1	Darreh Zar	BH-DZ51;279-281m	Phyllic	0.42	0.002	0.040	-
DZP-2	Darreh Zar	BH-DZ51;281-288m	Potassic+Phyllic	0.46	0.010	0.050	0.34
DZP-3	Darreh Zar	BH-DZ51;292-294m	Potassic+Phyllic	0.43	0.012	0.040	0.38
DZP-4	Darreh Zar	BH-DZ51;188-191m	Phyllic	0.51	0.030	0.020	-
DZP-5	Darreh Zar	BH-DZ51;152-156m	Phyllic	0.48	0.010	0.030	-
DZP-6	Darreh Zar	Outcrop	Phyllic	0.40	0.028	0.050	-
DZP-7	Darreh Zar	Outcrop	Phyllic	0.45	0.021	0.030	-
DZP-8	Darreh Zar	Outcrop	Phyllic	0.46	0.024	0.030	-
DZP-9	Darreh Zar	Outcrop	Phyllic	0.34	0.022	0.040	-
DZP-10	Darreh Zar	BH-DZ51;252-257m	Phyllic	0.43	0.021	0.030	-
SCP-1	Sar Cheshmeh	BH-979;175-179m	Propylitic	0.29	0.001	0.017	-
SCP-2	Sar Cheshmeh	BH-979;179-184m	Propylitic	0.26	0.001	0.016	-
SCP-3	Sar Cheshmeh	BH-979;185-186m	Propylitic	0.22	0.000	0.029	-
SCP-4	Sar Cheshmeh	BH-986;82.5-90m	Weakly Biotitized	0.18	0.003	0.006	0.48
SCP-5	Sar Cheshmeh	BH-979;90-91.7m	Weakly Biotitized	0.22	0.006	0.009	0.38
SCP-6	Sar Cheshmeh	BH-979;102-105m	Weakly Biotitized	0.27	0.011	0.017	0.33
SCP-7	Sar Cheshmeh	BH-979;108-110m	Weakly Biotitized	0.12	0.005	0.010	0.36
SCP-8	Sar Cheshmeh	BH-1006;195-198m	Intensely Biotitized	0.52	0.016	0.036	0.46
SCP-9	Sar Cheshmeh	BH-1006;200-204m	Intensely Biotitized	0.54	0.009	0.035	0.43
SCP-10	Sar Cheshmeh	BH-991;436-438m	Intensely Biotitized	0.52	0.015	0.069	0.55
SCP-11	Sar Cheshmeh	BH-991;438-439.8	Intensely Biotitized	1.32	0.048	0.074	0.48
SCP-12	Sar Cheshmeh	BH-991;439.8-440m	Intensely Biotitized	1.16	0.038	0.094	0.59
SCP-13	Sar Cheshmeh	BH-991;440-442m	Intensely Biotitized	0.9	0.036	0.022	0.39
SCP-14	Sar Cheshmeh	Outcrop	Intensely Biotitized	1.04	0.043	0.048	0.53
SCP-15	Sar Cheshmeh	Outcrop	Intensely Biotitized	1.07	0.084	0.046	0.49
SCP-16	Sar Cheshmeh	Outcrop	Intensely Biotitized	0.85	0.040	0.047	0.47
SCP-17	Sar Cheshmeh	BH-991;220-225m	Intensely Phyllic±Argillic	1.22	0.040	0.089	-
SCP-18	Sar Cheshmeh	BH-991;247-248m	Intensely Phyllic±Argillic	1.21	0.057	0.120	-
SCP-19	Sar Cheshmeh	BH-997;260-263.5	Intensely Phyllic±Argillic	0.78	0.088	0.020	-
SCP-20	Sar Cheshmeh	BH-997;268-271m	Intensely Phyllic±Argillic	0.53	0.196	0.049	-
SCP-21	Sar Cheshmeh	BH-997;271-278m	Intensely Phyllic±Argillic	0.39	0.180	0.051	-
SCP-22	Sar Cheshmeh	BH-997;278-284m	Intensely Phyllic±Argillic	0.43	0.500	0.024	-
SCP-23	Sar Cheshmeh	BH-997;290-292.5	Intensely Phyllic±Argillic	1.09	0.063	0.040	-
SCP-24	Sar Cheshmeh	BH-1000;391-394m	Intensely Phyllic±Argillic	0.36	0.145	0.040	-
SCP-25	Sar Cheshmeh	BH-1003;554-564m	Intensely Phyllic±Argillic	0.29	0.002	0.017	-
SCP-26	Sar Cheshmeh	BH-1002;606-609m	Intensely Phyllic±Argillic	0.7	0.014	0.055	-
SCP-27	Sar Cheshmeh	BH-1002;615-618m	Intensely Phyllic±Argillic	0.54	0.067	0.038	-
SCP-28	Sar Cheshmeh	BH-1002;638-642m	Intensely Phyllic±Argillic	0.57	0.067	0.024	-
SCP-29	Sar Cheshmeh	BH-1002;643.5-646m	Intensely Phyllic±Argillic	1.28	0.007	0.091	-
SCP-30	Sar Cheshmeh	BH-1002; 646.5-651m	Weakly Phyllic±Argillic	0.34	0.057	0.020	-
SCP-31	Sar Cheshmeh	Outcrop	Weakly Phyllic±Argillic	0.39	0.058	0.025	-
SCP-32	Sar Cheshmeh	Outcrop	Weakly Phyllic±Argillic	0.41	0.086	0.024	-
SCP-33	Sar Cheshmeh	Outcrop	Weakly Phyllic±Argillic	0.43	0.074	0.056	-
SCP-34	Sar Cheshmeh	BH-1003;781-793m	Weakly Phyllic±Argillic	0.22	0.003	0.013	-
SCP-35	Sar Cheshmeh	BH-1003;795-800m	Weakly Phyllic±Argillic	0.27	0.009	0.028	-
SCP-36	Sar Cheshmeh	BH-1003;850-860m	Potassic±Phyllic	0.15	0.002	0.0١۵	0.39
SCP-37	Sar Cheshmeh	BH-1003;860-870m	Potassic±Phyllic	0.26	0.001	0.010	0.43
SCP-38	Sar Cheshmeh	BH-1003;870-880m	Potassic±Phyllic	0.03	0.001	0.0١٠	0.38
SCP-39	Sar Cheshmeh	BH-1003;880-890m	Potassic±Phyllic	0.25	0.000	0.016	0.39
SCP-40	Sar Cheshmeh	BH-1003;890-900m	Potassic±Phyllic	0.6	0.008	0.030	0.36

Table 3. The average Au, Mo, Cu and magnetite contents together with Cu/Au (atomic) and Au/Mo ratios in some porphyry copper deposits from Kerman region compared with different type of porphyry copper deposits [4,6]

Ore deposit	Au (g/t)	Mo (%)	Cu (%)	Cu/Au (atomic ratio)	Au/Mo	Fe_3O_4 (%)
Sar Cheshmeh	0.040	0.050	0.65	504061	0.80	0.40
Meiduk	0.053	0.006	0.67	392145	8.83	0.79
Darreh Zar	0.036	0.018	0.44	379135	2.00	–
Sar Kuh	0.083	0.003	0.33	123328	27.00	1.24
Dar Alu	0.031	0.007	0.44	440286	4.42	–
Sara	0.034	0.005	0.37	337556	6.80	–
Abdar	0.072	0.013	0.30	129247	5.50	0.80
Seridun	0.024	0.011	0.26	336034	2.18	–
Porphyry Cu-Mo	0.12	0.016	0.41	>>40000	<3	0.05
Porphyry Cu-Au-Mo	0.15	0.015	0.48	–	3-30	1
Porphyry Cu-Au	0.38	0.003	0.55	<40000	>30	2.6

associated with copper. It appears that gold has been introduced with copper during the earliest stage of alteration and mineralization. The highest copper and gold grades commonly coincide in central part of the deposits (potassic zone), and there is a strong positive correlation between Au and Cu. Kesler *et al.*, [6] indicated that gold in porphyry copper deposits commonly is carried by bornite and chalcopyrite where they are sufficiently abundant. In deposits that contain abundant bornite, it is the preferred host for gold. Where bornite is rare or absent in the early alteration and mineralization stage, gold is associated with chalcopyrite [38,40-42]. In porphyry copper deposits, gold is found mainly as native grains in the form of inclusions in Cu-Fe-S sulfides, but more commonly it is found along their grain margins. The experimental data have indicated that bornite and chalcopyrite in many porphyry copper deposits are saturated with gold between about 700 and 400°C [6,10]. Since this temperature range is considerably higher than those at which porphyry copper deposits commonly form, many of the above mentioned researchers believed that gold originally have been deposited as solid solution in Cu-Fe-S sulfides when the porphyry copper deposits formed at high-temperature (700-600°C), and then exsolved to concentrate along sulfide grain boundaries at the temperatures typical of ore deposition (400-250°C). The extent of such solid solution can be evaluated with recent experimental data on the solubility of gold in high-temperature phases in the Cu-Fe-S systems, especially in bornite rather than chalcopyrite [10]. Kesler *et al.*, [6] noted that if ore-forming fluids starts deposition at 700°C, the gold saturated Cu-Fe-S sulfides will contain 800 ppm gold. This will decrease to 200 ppm at 600°C.They believed that this decrease in temperature of about 100°C could release almost 75% of the gold in the Cu-Fe-S sulfides. Also, they indicated that if ore deposition started at 600°C with bornite-chalcopyrite assemblage to form chalcopyrite-bornite-pyrite at lower temperature

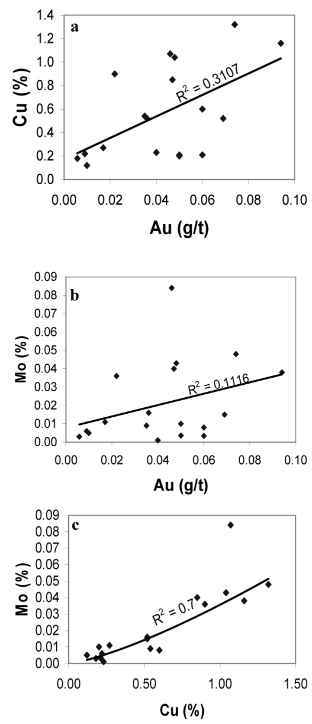

Figure 3. Correlation between Au and Cu (a), Au and Mo (b), and Mo and Cu (c) in potassic-ore samples from Kerman porphyry copper deposits.

alteration-mineralization stage (400-200°C), this drop in temperature could release only 200 ppm gold from Cu-Fe-S sulfide solid solution. These relations not only indicate that the Au-content in high-temperature ore-forming fluids will be more due to higher solubility of gold but also suggest that Au is exsolved from Cu-Fe-S sulfides during the cooling of deposits. Fluid inclusion and sulfur isotope studies in Sar Cheshmeh and Meiduk deposits showed maximum ore depositional temperatures between 600 and 400°C [21,34]. Therefore, we can assume that the highest temperature of ore-forming fluids in these ore deposits was less than 600°C. Considering these temperatures and based on the observed positive correlation between Cu and Au in ores samples from the potassic zones (Fig. 3), the presence of gold in the structure of chalcopyrite and also as independent phases in Sar Cheshmeh deposit [48], suggest that gold had originally been substituted for copper in the relatively high-temperature Cu-Fe-S sulfides and then exsolved from chalcopyrite due to decrease in temperature from 600°C to 250°C. This is in line with the experimental data of Simon *et al.*, [10] and Kesler *et al.*, [6]. Therefore, it seems the low content of gold in the Kerman porphyry copper deposits can be the result of the originally Au-poor hydrothermal fluids due to their low temperature which let little gold to enter the structure of the early formed Cu-Fe-S sulfides (chalcopyrite). The low temperature of the early ore-forming fluids for the Kerman porphyry copper deposits can be confirmed by the low content of higher temperature Cu-Fe-S sulfides such as bornite. Furthermore, Nedimovic [24] based on paragenesis of ore minerals have classified Kerman porphyry copper deposits as deposits generated in moderate temperature [24]. Simon *et al.*, [10] noted that primary porphyry copper deposits that form at low temperatures (below about 500°C) will consist dominantly of chalcopyrite and pyrite. These deposits will contain less gold, which is hosted by chalcopyrite relative to higher temperature porphyry copper deposits which contain more gold which is closely associated with bornite and magnetite.

According to Kesler, *et al.* [6], one of the most important processes which influence the gold content in the porphyry copper ore bodies, is the late events of mineralization which cause the remobilization of deposited copper and gold through destruction of bornite and chalcopyrite in high temperature (potassic) zone. Studies have shown that the late high-temperature hydrothermal processes which are recognized by the presence of quartz-sericite assemblage in phyllically altered rocks caused the Cu to remobilize more than Au in comparison with low-temperature hydrothermal processes (carbonate-sericite assemblage) [6]. Presence

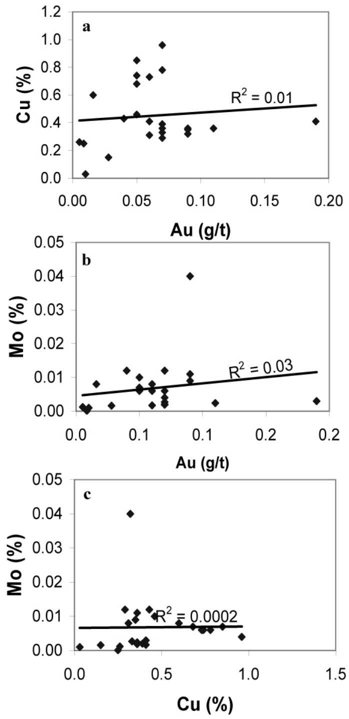

Figure 4. Correlation Au and Cu (a), Au and Mo (b), and Mo and Cu (c) in potassically altered rocks affected by phyllic alteration from Kerman porphyry copper deposits.

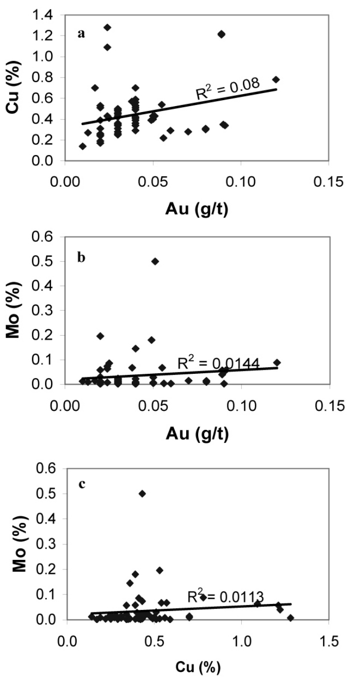

Figure 5. Correlation between Au and Cu (a), Au and Mo (b), and Mo and Cu (c) in strongly phyllic-ore samples from Kerman porphyry copper deposits.

of pervasive and high temperature quartz-sericite-pyrite alteration (350°C-300°C; [21,34]) in the Kerman porphyry copper deposits [17-19,21,34,50], the high Cu concentrations (and Cu/Au ratio) in potassic-phyllic ores, along with the poor correlation between Au and Cu (Figs. 4 and 5) indicates different behavior of Cu and Au in response to relatively high-temperature ore-forming solutions (350°C-250°C; [21,34]) in the middle and late stages of ore-deposition (phyllic zone). It seems that the Cu re-mobilized during the destruction of early formed Cu-Fe sulfides by the late stage ore-forming solutions, was re-deposited along with quartz-sericite mineral assemblage which overprinted potassic zone. This is supported by the similarity of lead isotope composition of early ($^{206}Pb/^{204}Pb$ = 18.53-18.59, $^{207}Pb/^{204}Pb$ = 15.59-5.61, $^{208}Pb/^{204}Pb$ = 38.59-38.69) and late sulfides ($^{206}Pb/^{204}Pb$=18.57-18.61, $^{207}Pb/^{204}Pb$ = 15.60-15.65, $^{208}Pb/^{204}Pb$ = 38.66-38.82) in Kerman region [25]. This late stage process caused an increase in Cu concentration in the potassically altered rocks which were overprinted by the phyllic alteration (*e.g.*, Cu grades up to 1.4% in biotitized rocks affected by phyllic alteration in Sar Cheshmeh deposit) [17,33,50].

Kesler *et al.*, [6] believes that gold might be scavenged from Cu-Fe-S solid solution by later, low-temperature ore-forming solutions. This process would lead to the release of free particles of gold and its dispersion in the whole ore body or concentration of gold in polymetal and epithermal veins outside the Cu ore zone. This process can explain the presence of Au in the form of free particles in the whole ore body [48] and its presence within the epithermal as well as polymetal veins in country rocks surrounding the porphyry copper systems in Sar Cheshmeh [50], Abdar [21], and Meiduk deposits [24].

The low grades of Au in the Kerman porphyry copper deposits can be explained by their derivation from originally Au-poor magmatic and hydrothermal fluids. Gold which is not accommodated within the chalcopyrite at low temperature (phyllic zone), will probably be associated with pyrite as well as in the form of free gold grains and also associated with epithermal veins which are scattered outside the copper ore zone [10,51]. Many Au-poor porphyry copper deposits in southwest USA, Central Asia, and west of South America are associated with widespread phyllic alteration, implying that the low temperature hydrothermal solutions responsible for the phyllic alteration removed the gold from the central parts of the porphyry systems. The remobilized Au is concentrated as epithermal veins in the country rocks [6,49,52-54].

Magnetite Content

Magnetite is a common mineral of the potassic alteration assemblage in the porphyry copper ores [55]. The magnetite content of the potassic zones ranges between 0.05 and 10 percent [4]. Sillitoe [3] and Cox

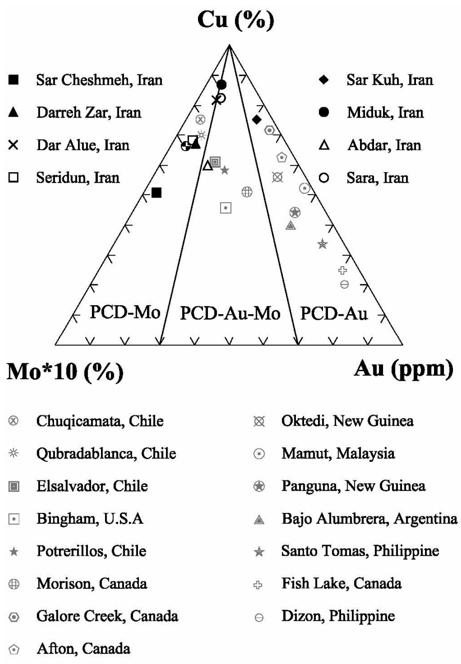

Figure 6. plots of Kerman porphyry copper deposits on the Cu-Mo-Au discrimination diagrams of Cox and Singer [4]. Data for other deposits derived from Vila and Sillitoe [73].

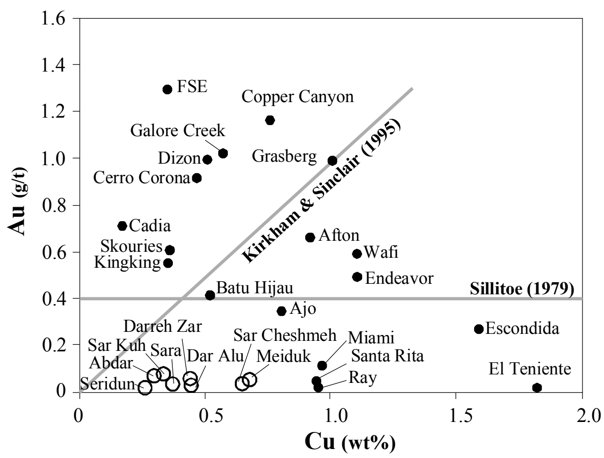

Figure 7. Location of the Kerman porphyry copper deposits on Cu vs. Au diagram on which the porphyry Cu-Au deposits are plotted above the diagonal line of Kirkham and Sinclair [6] and the horizontal line of Sillitoe [3].

and Singer [4] have proven a strong positive correlation between magnetite and gold contents of the porphyry copper deposits. The high magnetite content (3-10 wt.%) indicates high oxidation condition of the ore-forming fluids responsible for gold and copper mineralization in the gold-rich porphyry copper deposits [3,4]. The low gold grades in the Kerman porphyry copper deposits are consistent with the low magnetite content in the potassic zones. The magnetite contents (wt.%) in the potassic ore samples from the Kerman deposits are as follows (Table 3): Sar Kuh ,1.24 wt.%; Abdar ,0.80 wt.%; Meiduk, 0.79 wt.%; and Sar Cheshmeh ,0.4 wt.%. These values are similar to those of the gold-poor porphyry copper deposits (≤1wt.%) [4]. Although both Au and magnetite contents are low but interestingly our data indicate that there is a significant positive correlation (r=0.93) between average Au grades and average magnetite content of the potassic ores in some porphyry copper deposits of the Kerman region (Fig. 8). This reflects the higher fO_2/fS_2 of ore-forming fluids in deposits with higher gold and magnetite contents (*i.e.*, Sar Kuh, Abdar and Meiduk) compared with the gold-poor deposits (*i.e.*, Sar Cheshmeh and Darreh Zar). One possible mechanism for maintaining high fO_2/fS_2 during the early gold-deposition stage (*i.e.*, potassic alteration), might be the dissociation of H_2O to H_2 and O_2 [4,56]. This process would be favored by the high temperature and low pressure that would be associated with quartz diorite and other intrusions emplaced at high levels in the crust [4]. Escape of the smaller hydrogen molecules would result in the high fO_2/fS_2 required to form magnetite and restrict gold mobilization [4]. The high magnetite content in the center of porphyry systems can be significant as an exploration tool for exploring gold-rich porphyry copper deposits [3,10,11,57].

Emplacement Depth

According to Cox and Singer [4] there is a significant negative correlation (r=-0.90) between gold content and emplacement depth of porphyry copper deposits. They showed that gold-rich porphyry copper deposits tend to be emplaced at very shallow levels (0.4-1.5 km) in the crust relative to the gold-poor porphyry copper deposits (3.6-4.6 km). Etminan [34] and McInnes *et al.*, [33] showed that Sar Cheshmeh deposit was emplaced at depth between 4 and 5 km. Also, McInnes *et al.* [33] estimated a depth of 2.8 and 2.5 km for emplacement of Abdar and Meiduk deposits, respectively. The shallow emplacement depth of the Abdar and Meiduk deposits together with their higher gold contents compared to Sar Cheshmeh that is characterized by lower Au content (average 0.04 g/t) and deeper emplacement, indicates a negative correlation between emplacement depth and the amount of gold in the Kerman porphyry copper deposits. The higher level emplacement of gold-rich porphyry copper deposits may cause the high oxidation conditions (SO_2/H_2S>1) of ore-forming fluids [49]. This condition increases Au solubility in hydrothermal fluids which finally form the Au-rich porphyry copper deposits [49]. In the deeply emplaced deposits (3-5 kilometers), abundant occurrence of pyrite indicates reduced conditions in the magmatic-hydrothermal system(high fS_2/fO_2), in this situation, gold will be transported as bi-sulfide complexes in hydrothermal fluids [49], and can migrate to the peripheral zones of porphyry systems where the gold-rich epithermal veins are formed.

Tectonic Setting

Although, the tectonic setting appears to be one of the most important factor that controls the gold content of porphyry copper deposits [1,8], but it is not generally considered as a critical factor [2,3,7,9,11]. Island arc hosted porphyry copper deposits (*e.g.*, Santo Tomas, Dizon, Kingking) have elevated Au content in comparison with the continental margin porphyry copper deposits (Escondida, Morenci, santa Rita)[1,6]. The Kerman porphyry copper region is located on the southeastern segment of subduction/collision-related Urumieh-Dokhtar magmatic arc constructed on the southeastern margin of the central Iranian continental

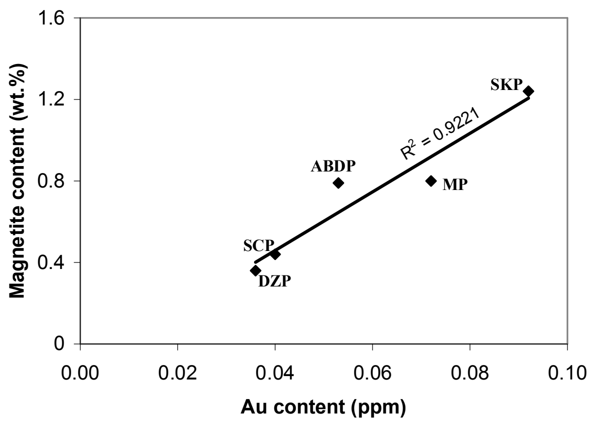

Figure 8. Plots of the average magnetite contents of the potassic zone against the average gold grades for the Kerman porphyry copper deposits. The correlation coefficient is 0.98. ABDP=Abdar porphyry copper prospect; DZP= Darreh Zar porphyry copper deposit; MP=Meiduk porphyry copper deposit; SCP=Sar Cheshmeh porphyry copper deposit; SKP=Sar Kuh porphyry copper prospect.

block [21,22,25,26]. Geochemical and isotopic signature (Sr, Nd and Pb) of Kerman ore-hosting intrusions indicated that productive adakitic-like magmas and associated metals (Cu) originated from the melting of the lower crustal mafic rocks rather than the melting of the subducting hot slab (Fig. 2f) [25,26]. Mungall [58] believes that adakitic magmas which have been formed as the direct melting of subducting oceanic slab due to their higher temperature and the remarkable higher oxygen fugacity, in comparison to those which have been originated from melting of thickened lower crustal rocks, have a considerable potential to generate Au-rich porphyry copper deposits. Due to the lower temperature and the lower oxygen fugacity of the Kerman ore-hosting magmas, the porphyry copper deposits cannot be enriched in gold [58]. This characteristic also seems to comply with Kessler's opinion [1] regarding the low Au content of porphyry copper deposits generated in continental margin arcs.

Other Signatures of the Gold-Poor Porphyry Copper Deposits

One of the most important features which will support the gold-poor nature of Kerman porphyry copper deposits is the presence of a considerable amount of Mo-bearing ores in the copper ore zones [18, 34], and the lack of geochemical relationship between Au and Mo (Figs. 3 and 4). Sillitoe [3] believes that gold-rich porphyry copper deposits are Mo-free. Cox and Singer [4] proved a negative correlation between Au and Mo in porphyry copper deposits (r= -0.45). These might be attributed to the relatively low oxidation condition ($SO_2/H_2S<1$) of the ore-forming fluids responsible for formation of porphyry Cu-Mo deposits with respect to the gold-rich porphyry copper deposits [4,59-62]. Molybdenum is concentrated within both copper ore shell and the peripheral pyrite zones in the porphyry Cu-Mo deposits [4]. Gold would migrate to the surroundings of the system under the same circumstances and forms limited gold mineralization associated with epithermal and poly-metal veins [4].These features are observed in the porphyry copper deposits of the Kerman region and can indicate that such deposits are of porphyry Cu-Mo type. Recognition of a poly-metal vein with a high gold grade (0.5 g/t) outside the copper ore zone of Sar Cheshmeh deposit [50,63], as well as the presence of gold-rich poly-metal veins around Meiduk deposit (Chah Mesi deposit) [21,24] and Abdar deposit [21] are consistent with the scarcity of gold in the Kerman porphyry copper deposits.

Ore deposit morphology has been introduced as one of the criteria which can distinguish the Au-rich porphyry copper deposits from those of Cu-Mo or gold-poor deposits. Sinclair *et al.*, [9] applied the porphyry classification scheme of Sutherland Brown [64] for a group of porphyry deposits in the British Columbia and found out that porphyry copper-gold deposits tend to occur in two forms, namely classic-type and volcanic-type systems. According to this classification, the classic-type deposits are centered on small cylindrical plutons. They are commonly associated with breccia pipes and have concentric zones of alteration and mineralization, and coeval volcanic rocks are commonly absent. Volcanic-type deposits are related to irregular or dike-like igneous bodies that have intruded a coeval volcanic pile. In contrast, the plutonic-type porphyry deposits are characterized by mineralization as integral zones of medium-sized plutons having phaneritic texture. Cox and Singer [4] showed that all gold-rich porphyry copper deposits are grouped in the volcanic-type deposits in comparison with Mo-rich deposits which show classic-type or plutonic-type morphology. Considering the proposed classification and the geological and radiometric age data [15,17,19,21,25,26, 33,35,63,65], the porphyry copper deposits of the Kerman region formed in the late stages of arc development (middle-late Neogene), especially when volcanism ceased and a compressive tectonic regime prevailed. Moreover, and the lack of coeval volcanic rocks with the ore-hosting intrusions [25,26] and abundant occurrences of breccia pipes [36,50,65] at the site of ore deposition indicate that Kerman porphyry copper deposits belong to the classic-type of porphyry Cu deposits. This is consistent with Au-poor signature of porphyry copper deposits in the Kerman region.

Some researchers [1,2,9] have mentioned that tonnage of the Au-Cu porphyry deposits are far less than Cu-Mo deposits. Cox and Singer [4] confirmed the idea that the increase for ore-tonnage with decreases the amount of gold in porphyry copper deposits. They identified the Au-rich porphyry copper deposits have a tonnage of about 100 to 200 million tons or lower and Mo-rich porphyry copper deposits have a tonnage around 500 to 1000 million tons. Therefore, the lower tonnage of Au-rich porphyry copper deposits in comparison to Mo-rich porphyry copper deposits in a comprehensive worldwide scale is accepted by most of the researchers. Based on the existing data (Table 1), there is a negative correlation between tonnage and gold content of Kerman porphyry copper deposits. Deposits with lower tonnage (Abdar, Sar Kuh, Meiduk) are richer in gold compared with the giant Sar Cheshmeh deposit (Fig. 9). However, the gold grades are still at the level of gold-poor porphyry copper deposits.

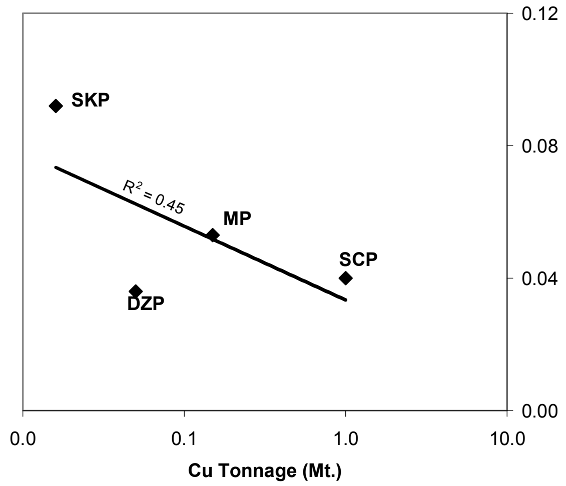

Figure 9. Inverse correlation between Cu-tonnage and average gold contents of Kerman porphyry copper deposits. Cu-tonnages are derived from Table 1. DZP= Darreh Zar porphyry copper deposit; MP=Meiduk porphyry copper deposit; SCP=Sar Cheshmeh porphyry copper deposit; SKP=Sar Kuh porphyry copper prospect.

Acknowledgments

We thank the NICICO for providing access to drill core samples of the Kerman porphyry copper deposits, as well as Au, Mo, Cu, and magnetite analyses. The authors acknowledge constructive reviews from three anonymous reviewers of the Journal of Sciences, Islamic Republic of Iran that helped to improve the manuscript.

References

1. Kesler S.E. Copper, molybdenum, and gold abundances in porphyry copper deposits. Econ. Geol., 68: 106-112 (1973).
2. Titley S.R. Copper, molybdenum, and gold content of some porphyry copper systems of the southwestern and western Pacific. *Econ. Geol*., 73: 977-981 (1978).
3. Sillitoe R.H. Some thoughts on gold-rich porphyry copper deposits. *Mineral. Deposita.*, 14: 161-174 (1979).
4. Cox D.P., and Singer D.A. Distribution of gold in porphyry copper deposits. *U.S.Geol.Surv.Bull*., 1877-C: C1-C14 (1988).
5. Kerrich R., Goldfarb R., Groves D., and Garwin S. The geodynamics of world-class gold deposits: characteristics, space time distribution and origins. In: Hagemann S.G., and Brown P.E. (Eds.), Gold in 2000. Soc. *Econ. Geol. Rev.,* 13:501-522 (2000).
6. Kesler S.E., Chryssoulis S.L., and Simon G. Gold in porphyry copper deposits: its abundance and fate. *Ore. Geol. Rev.,* 21:103-124 (2002).
7. Lowell J.D. Gold mineralization in porphyry copper deposits. *Soc. Min. Eng. Rep.*, 17; 88-117 (1989).
8. Hollister V.F. An appraisal of the nature and source of porphyry copper deposits. *Minerals. Sci. Eng.*, 7: 225-233 (1975).
9. Sinclair A.J., Drummond A.D., Carter N.C., and Dawson K.M. A preliminary analysis of gold and silver grades of porphyry-type deposits in western Canada. In: Levinson A.A. (Ed.), Precious metals in northern Cordillera. Assoc. *Explor. Geochem*., Rexdale, Ontario, p.157-172 (1982).
10. Sillitoe R.H. Characteristics and controls of the largest porphyry copper-gold and epithermal gold deposits in the circum-Pacific region. *Aust. J. Earth. Sci.,* 44: 373-388 (1997).
11. Simon G., Kesler S.E., Essene J., and Chryssoulis S. Gold in porphyry copper deposits: Experimental determination of the distribution of gold in the Cu-Fe-S system at 400°C to 700°C. *Econ.Geol.,* 95: 259-270 (2000).
12. Sillitoe R.H. Gold-rich porphyry deposits: Descriptive and genetic models and their role in exploration and discovery. *Soc. Econ. Geol. Rev.,* 13: 315-345 (2000).
13. Kirkham R.V., and Sinclair W.D. Porphyry copper, gold, molybdenum, tungsten, tin, and silver. In: Eckstrand O.R., Sinclair W.D., and Thorpe R.I. (Eds.), Geology of Canadian Mineral deposit types. *Geol. Surv. Can.,* 8:421-446 (1995).
14. Samani B. Distribution, setting and metallogenesis of copper deposits in Iran. In: Porter, T.M. (Ed.), Porphyry and hydrothermal copper and gold deposits: A global Perspective, Perth, 1998, Conference Proceedings: Glenside, South Australia, Aust. Min. Found., 135-158 (1998).
15. Rio Tinto Ltd. Interpretation of LANDSAT TM imagery, Kerman region, Iran. *Unpublished report of National Iranian Copper Industries Company*, 42p(2000).
16. Bazin D. and Hubner H. Copper deposits in Iran: Geol. Surv. Iran., 13, 232 p (1969).
17. Saric V. Mijalkovic N. Metallogenic map of Kerman region, 1:500000 scale. In: Exploration for ore deposits in Kerman region. *Geol. Surv. Iran. Rep*., 53, 247 p (1973).
18. Waterman G.C., and Hamilton R.L. The Sar-Cheshmeh porphyry copper deposit. *Econ.Geol.,* 70: 568-576 (1975).
19. Shahabpour J. Aspects of alteration and mineralization at the Sar Cheshmeh copper-molybdenum deposit, Kerman, Iran. Unpublished Ph.D. *Thesis,* University of Leeds, England, 342p (1982).
20. Shahabpour J., and Kramers J.D. Lead isotope data from the Sar Cheshmeh porphyry copper deposit, Kerman, Iran. *Mineral. Deposita*., 22: 278-281 (1987).
21. Hassanzadeh J. Metallogenic and tectono-magmatic events in the SE sector of the Cenozoic active continental margin of Iran (Shahr e Babak area, Kerman province). Unpublished Ph.D. *Thesis,* University of California, Los Angeles, 204p (1993).
22. Shahabpour J. Tectonic evolution of the orogenic belt in the region located between Kerman and Neyriz. *J. Asian. Earth. Sci.,* 24: 405-417 (2005).
23. Dimitrijevic M.D. Geology of Kerman region. *Geol. Surv. Iran. Rep*., 52: 334p (1973).
24. Nedimovic. Exploration for ore deposits in Kerman region. *Geol. Surv. Iran*. *Rep*., 53: 247p (1973).
25. Shafiei B. Metallogenic model of Kerman porphyry

copper belt and its exploratory approaches: Unpublished Ph.D. *Thesis,* Shaheed Bahonar University of Kerman, Iran, 311p (2008).
26. Shafiei B., Shahabpour J. and Haschke M., Transition from Paleogene normal calc-alkaline to Neogene adakitic-like plutonism and Cu-metallogeny in the Kerman porphyry copper belt: response to Neogene crustal thickening. *J. Sci. I. R. Iran.,* 19(1): 67-84 (2008).
27. Berberian F., Muir I.D., Pankhurst R.J., and Berberian M. Late Cretaceous and early Miocene Andean type plutonic activity in northern Makran and central Iran. *J. Geol. Soc. Lond.,* 139: 605-614 (1982).
28. Dercourt J., Zonenshain L., Ricou L.E., Kasmin G., LePichon X., Knipper A.L., Grandjacquet C., Sbortshikov I.M., Geyssant J., Lepvrier C., Pechersky D.H., Boulin J., Sibuet J.C, Savostin L.A., Sorokhtin O., Westphal M., Bazhenov M.L., Lauer J.P., and Biju-Duval B. Geological evolution of the Tethys belt from the Atlantic to Pamirs since the Lias. *Tectonophysics*, 123: 241-315 (1986).
29. Ricou LE., Tethys reconstructed: plates continental fragments and their boundaries since 260 Ma from Central America to south-eastern Asia. *Geodyn. Acta.,* 7: 169-218 (1994).
30. Mohajjel M., Fergusson C.L, and Sahandi M.R. Cretaceous-Tertiary convergence and continental collision, Sanandaj-Sirjan zone, western Iran. *J. Asian. Earth. Sci.,* 21: 397-412 (2003).
31. Agard P., Omrani J., Jolivet L., and Mouthereau F. Convergence history across Zagros (Iran): constraints from collisional and earlier deformation. *Int. J. Earth Sci.,* 94: 401-419 (2005).
32. Ghorashi-Zadeh M. Development of hypogene and supergene alteration and copper mineralization patterns, Sar Cheshmeh porphyry copper deposit, Iran. Unpublished M.Sc. *Thesis, Brock University., Canada,* 223p (1978).
33. McInnes B.I.A., Evans N.J., Fu F.Q., Garwin S., Belousova E., Griffin W.L., Bertens A., Sukama D., Permanadewi S., Andrew R.L., and Deckart K. Thermal history analysis of selected Chilean, Indonesian, and Iranian porphyry Cu-Mo-Au deposits. In: Porter TM.(Ed.), Supper porphyry copper and gold deposits: A global perspective, PGC publishing, Adelaide, 1-16 (2005).
34. Etminan H. Le porphyre cuprifere de Sar-Cheshmeh (Iran), role des phases fluids dans les mechanisms d'alteration et de mineralization. *Sci. Terr. Mem.,* 34, 78p (1977).
35. Shahabpour J. Some sulfide-silicate assemblages from the Sar Cheshmeh porphyry copper deposit, Kerman, I. R. Iran. *J. Sci. I. R. Iran.,* 11:39-48 (2000).
36. Shahabpour J. Unroofing fragmentites as a reconnaissance exploration tool in the central Iranian porphyry copper belt. *Econ. Geol*., 87: 1599-1606 (1992).
37. Jones B.K. Application of metal zoning to gold exploration in porphyry copper systems. *J. Geochem. Explor.,* 43:127-155 (1992).
38. Perrello J.A., Urzua F., Cabello J., and Ortiz F. Clustered, gold-bearing Oligocene porphyry copper and associated epithermal mineralization at La Fortuna, Vallenar region, northern Chile. In: Camus F., Sillitoe, R.H., and Peterson R. (Eds.), Andean Copper Deposits: New Discoveries, Mineralization, Style and Metallogeny. Soc. *Econ. Geol. Spe. Pub.,* 5:81-90 (1996).
39. Stanley C.R., Holbek P.M., Huyck H.L.O., Lang J.R., Preto V.A.G., Blower S.J., and Bottaro. Geology of the Copper mountain alkali porphyry copper-gold deposits, Princeton, British Columbia. In: In: Schroeter T.G. (Ed.), Porphyry deposits of the Northwestern Cordillera or North America. *Can. Inst. Min. Metal. Petr.,* 46:537-564 (1995).
40. Rebagliati C.M., Bowen B.K., Dopeland D.J., and Niosi C.W.A. Kemess South and Kemess North porphyry gold-copper deposits, northern British Columbia. In: Schroeter T.G. (Ed.), Porphyry deposits of the Northwestern Cordillera or North America. *Can. Inst. Min. Metal. Petr.,* 46:377-396 (1995).
41. Bouley B.A., George S.T.P., and Wetherbee P.K. Geology and discovery at Pebble Copper, a copper-gold porphyry system in southwest Alaska. In: Schroeter TG., (Ed.), Porphyry deposits of the Northwestern Cordillera or North America. *Can. Inst. Min. Metal. Petr.,*46:422-435 (1995).
42. Ulrich T., Gunthur D., and Heinrich C.A. The evolution of a porphyry Cu-Au deposit, based on LA-ICP-MS analysis of fluid inclusions: Bajo de la Alumbrere, Argentina. *Econ. Geol.,* 96:1743-1775 (2002).
43. Baldwin J.T., Swain H.D., and Clark G.H. Geology and grade distribution at the Panguna porphyry copper deposit, Bougainville, Papua New Guinea. *Econ. Geol.,* 73:690-702 (1978).
44. Cuddy A.S., and Kesler S.E. Gold in the Granisle and Bell porphyry copper deposits. In: Levinson, A., (Ed.), Precious metals in the Northern Cordillera. *Ass. Explor. Geochem. Spe.* 2:139-155 (1982).
45. Tarkian M., and Koopmann G. Platinum-group minerals in the Santo Tomas II (Philex) porphyry copper-gold deposit, Luzon Island, Phillippines. *Mineral. Deposita*., 30: 39-47 (1995).
46. Ballantyne G.H., Smith T.W., and Redmond P.B. Distribution and mineralogy of gold and silver in the Bingham Canyon porphyry copper deposit, Utah. In: John D.A., and Ballantyne G.H. (Eds.), Geology and ore deposits of the Oquirrh and Wasatch Mountains, Utah. *Soc. Econ. Geol. Guidebook.,* 29:147-153 (1997).
47. Rubin J.N., and Kyle J.R. Precious metal distribution in porphyry, skarn and replacement-type ore deposits of the Ertsberg district, Irian Jaya, Indonesia. *Econ. Geol.,* 92:535-551 (1997).
48. Salari Rad M.M., Tsunekawa M., Hirajima T., and Yoneda T. Gold occurrence in the Sar Cheshmeh porphyry copper ore and its behavior during beneficiation.In: *Proceeding of Copper 99-Cobre 99*, II-129-143 (1999).
49. Gammons C.H., and Williams-Jones A.E. Chemical mobility of gold in the porphyry-epithermal environment. *Econ. Geol*., 92:45-59 (1997).
50. Shafiei B., Shahabpour J., and Sadloo M. Geochemical characteristics, nature, and genesis of hypogene gold and silver in the Sar Cheshmeh porphyry copper deposit, Kerman. *J. Earth Sci*., 8:34-50 (2001).
51. Scaini M.J., Bancroft G.M., and Knips S.W. Reactions of

aqueous Au^{+1} sulfide species with pyrite as a function of pH and temperature. *Am. Mineral.,* 83:316-322 (1998).
52. Nielsen R.L. Hypogene texture and mineral zoning in a copper-bearing granodiorite stock, Santa Rita, New Mexico. *Econ. Geol.,* 63:37-50 (1968).
53. Reynolds J.T., and Bean R.E. Evolution of hydrothermal fluid characteristics at the Santa Rita, New Mexico, porphyry copper deposit. *Econ. Geol.,* 80:1328-1347(1985).
54. Casselman M.J., McMillan W.J., and Newman K.M. Highland Valley porphyry copper deposits near Kamloops, British Columbia: a review and update with emphasis on the Valley deposit. In: Schroeter T.G. (Ed.), Porphyry deposits of the Northwestern Cordillera or North America. *Can. Inst. Min. Metal. Petr.,* 46:161-191(1995).
55. Meyer C., and Hemley J.J. Wall-rock alteration. In: Barnes H.L. (Ed.), *Geochemistry of hydrothermal ore deposits*. Holt, Rinehart, and Winstone, New York., 670 p. (1967).
56. Ishihara S. The Granitoid Series and Mineralization. *Econ. Geol.,* 75:458-484 (1981).
57. Edwards R., and Atkinson K. *Ore Deposits Geology*. Chapman and Hall Company, 466 p (1985).
58. Mungall E.J. Roasting the mantle: slab melting and the genesis of major Au and Au-rich Cu deposits. *Geology*, 30: 915-918 (2002).
59. Kosaka H., and Wakita K. Some geologic features of the Mamut porphyry copper deposits, Sabah, Malaysia. *Econ. Geol.,* 73: 618-627(1978)
60. Seward T.M. The transport and deposition of gold in hydrothermal systems. In: Forster RP. (Ed.), Gold'82: The Geology, Geochemistry and Genesis of Gold Deposits. Proc. Sym. Harare, Zimbabwe 1982 Balkema, Rotterdam, 167-181 (1984).
61. Cameron E.M., and Hattori K. Archean gold mineralization and oxidized hydrothermal fluids. *Econ. Geol.,* 82:1177-1191 (1987).
62. Sillitoe R.H., Gold-rich porphyry copper deposits: Geological model and exploration implications. In: Kirkham R.V., Sinclair W.D., Thorpe R.I., and Duke J.M. (Eds.), Mineral deposit modeling. *Geol. Assoc. Can. Spec. Pap.,* 40: 465-478 (1993).
63. Shafiei B. The study of occurrence, geochemical distribution, and metallogenetic model of gold and silver in the Sar-Cheshmeh porphyry copper deposit. Unpublished M.Sc. *Thesis,* Shaheed Bahonar University of Kerman, Iran, 385p (2000).
64. Sutherland Brown A. Porphyry Deposits of the Canadian Cordillera. *Can. Inst. Min. Metall. Spec.,* 15: 7-16 (1976).
65. Shahabpour J. Post-mineralization breccia dike from the Sar Cheshmeh porphyry copper-molybdenum deposit, Kerman, Iran. *Explor. Min. Geol*., 3:39-43 (1994).
66. Porter M. An overview of the world's porphyry and other hydrothermal Cu and gold deposits and their distribution. In: Porter M. (Ed.), Porphyry and hydrothermal Cu and gold deposits: A global perspective. Perth, Conf Proc, Glenside, South Australia, Aus Min Found: 3-17(1998).
67. Maniar P.D., and Piccolli P.M. Tectonic discrimination of granitoids. *Geol. Soc. Am. Bull.,* 101: 635-643 (1989).
68. White A.J.R., and Chappel B.W. Granitoid types and their distribution in Lachlan fold belt, southeastern Australia. In: Roddick JA. (Ed.), Circum-Pacific plutonic terrains. *Geol. Soc. Am. Mem.,* 159: 21-34 (1983).
69. Defant M.J., and Drummond M.S. Derivation of some modern magmas by melting of young subducted lithosphere. *Nature*, 347: 662-665 (1993).
70. Whalen J.B., Currie K.L., and Chappel B.W. A-type granites: geochemical characteristics, discrimination and petrogenesis. *Contrib. Mineral. Petrol.,* 95: 407-419 (1987).
71. Batchelor R.A., and Bowden P. Petrogenetic interpretation of granitoid rock series: using multinational parameters. *Chem. Geol.,* 48: 43-55 (1985).
72. Wang Q, Wyman DA, Xu JF, Zhao ZH, Jian P, Xiong XL, Bao ZW, Li CF, Bai ZH (2006a) Petrogenesis of Cretaceous adakitic and shoshonitic igneous rocks in the Luzong area, Anhui Province (eastern China): Implications for geodynamics and Cu-Au mineralization. Lithos 89: 424-446.
73. Vila T., and Sillitoe R.H. Gold-rich porphyry systems in the Maricunga belt, northern Chile. *Econ. Geol*., 86: 1238-1260 (1991).